Supplementary Information

Stretchable Separator/Current Collector Composite for Superior Battery Safety

Zhikang Liu[1]†, Yanhao Dong[2,]†, Xiaoqun Qi[3], Ru Wang[1,4,5], Zhenglu Zhu[1], Chao Yan[4,5], Xinpeng Jiao[5], Sipei Li[2], Long Qie[1,3,*], Ju Li[2,6,*], and Yunhui Huang[3,*]

[1] Institute of New Energy for Vehicles, School of Materials Science and Engineering, Tongji University, Shanghai 201804, China

[2] Department of Nuclear Science and Engineering, Massachusetts Institute of Technology, Cambridge, MA 02139, USA

[3] State Key Laboratory of Material Processing and Die & Mold Technology, School of Materials Science and Engineering, Huazhong University of Science and Technology, Wuhan, Hubei 430074, China

[4] Nanjing Tongning Institute of New Materials, Nanjing, Jiangsu 211161, China

[5] Zhejiang Rouzhen Technology Co., Ltd., Jiaxing, Zhejiang 314499, China

[6] Department of Materials Science and Engineering, Massachusetts Institute of Technology, Cambridge, MA 02139, USA

Table of contents

Supplementary Figures S1-S9 Page S2-S10

Supplementary Tables S1-S4 Page S11-S14

Captions of Supplementary Videos S1-S9 Page S15

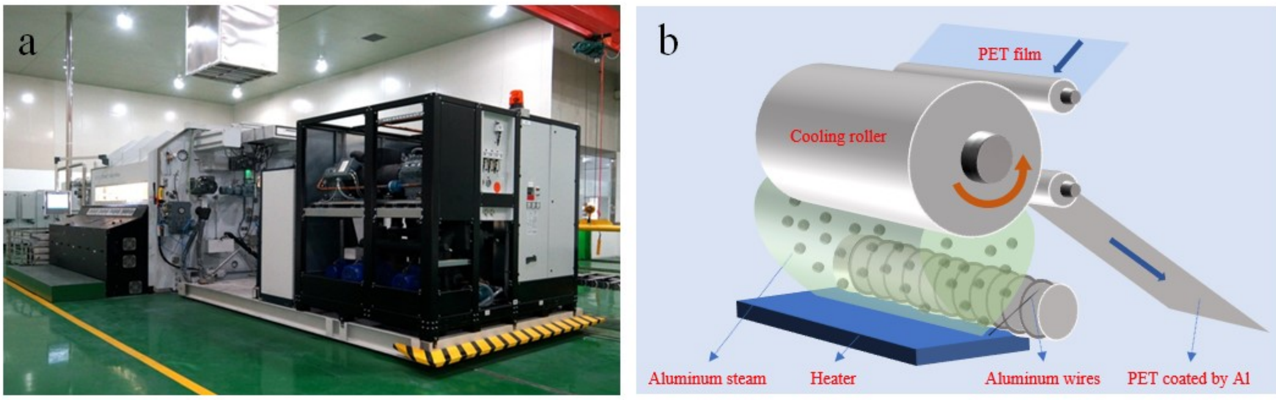

Supplementary Figure S1 (a) The vacuum-metallizing machine used and (b) the schematic of Al deposition for the roll-to-roll preparation of Al-PET.

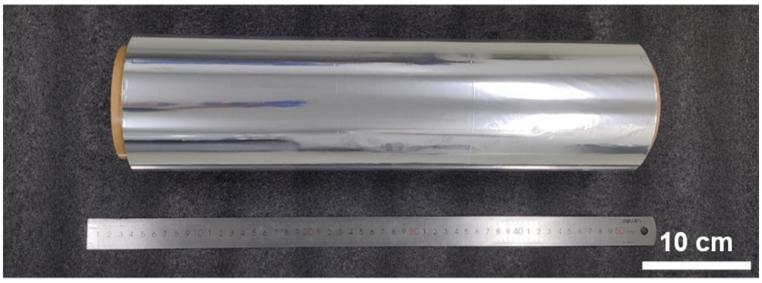

Supplementary Figure S2 Photo of the roll-to-roll processed Al-PET. The current daily production capacity of Al-PET by one vacuum-metallizing machine as shown in **Supplementary Figure S1a** is ~ 8000 m^2.

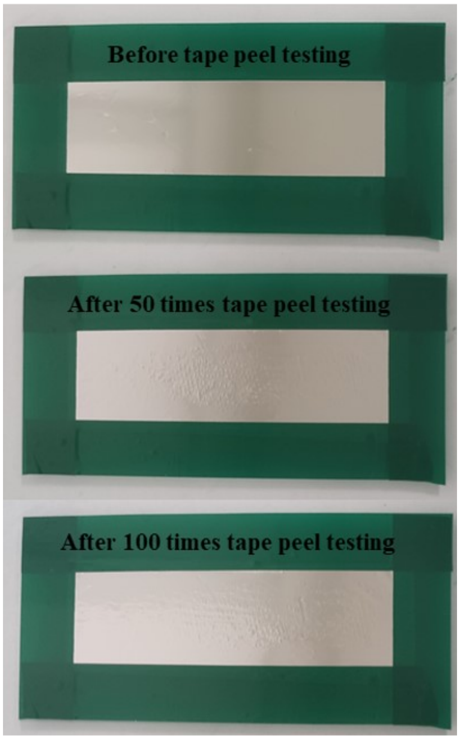

Supplementary Figure S3 Photos of Al-PET before tape peel testing, and after 50 and 100 times. Al-PET was fixed with green tapes around it and then subjected to a peeling test with 3M tape.

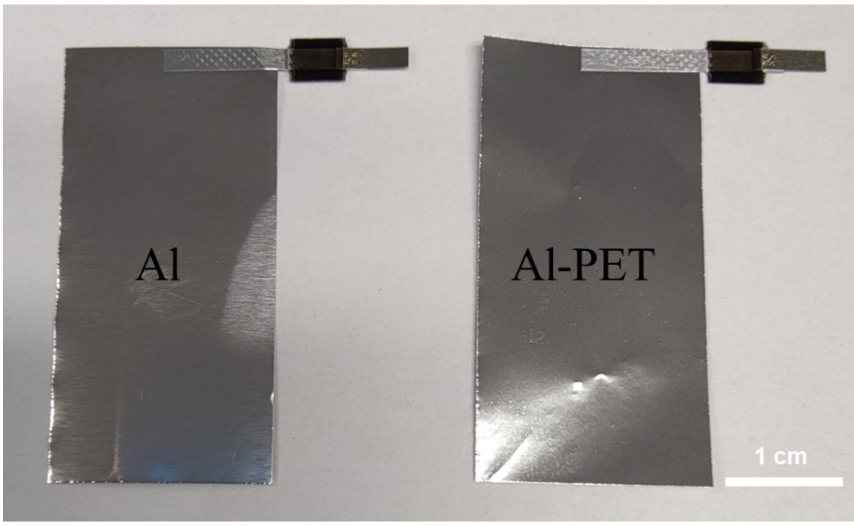

Supplementary Figure S4 Photos of Al and Al-PET SCCs after welding tabs.

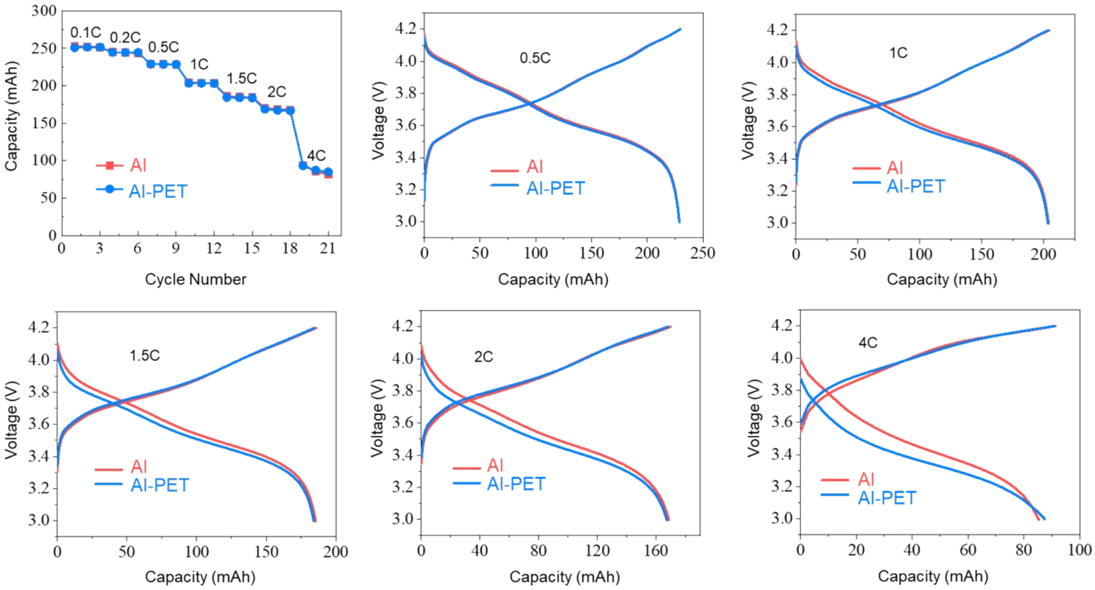

Supplementary Figure S5. Punch-cell rate performance and charge/discharge curves using 14 μm Al CC (labeled as Al) and Al-PET CC with 900 nm Al layer (labeled as Al-PET).

Supplementary Figure S6. Morphology of Al-PET stored in EC/DEC electrolyte at 25 ^{o}C and 60 ^{o}C for 72 h.

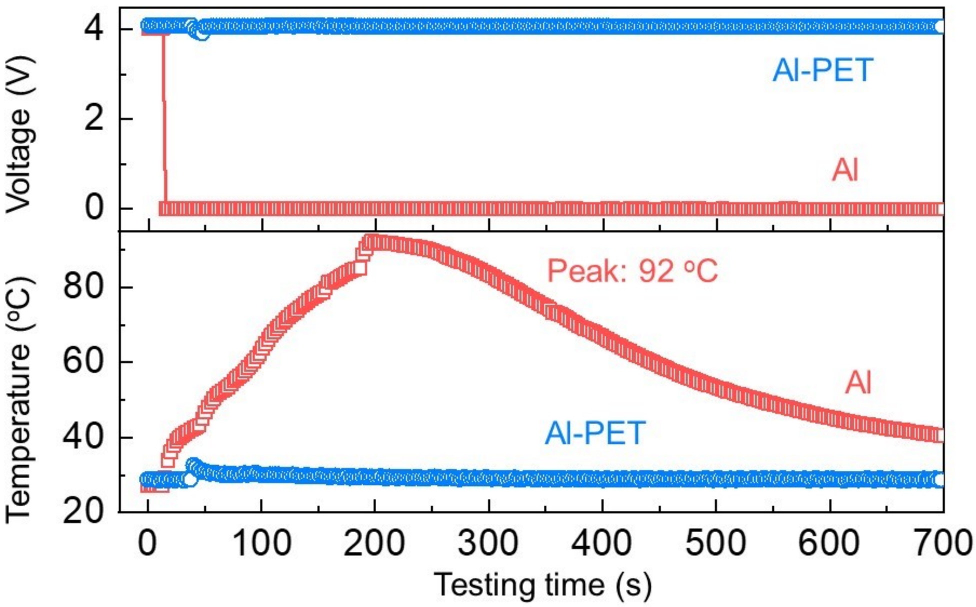

Supplementary Figure S7 Voltage and temperature (measured by a thermocouple) of 244 mAh pouch cells using Al and Al-PET SCCs during impact tests.

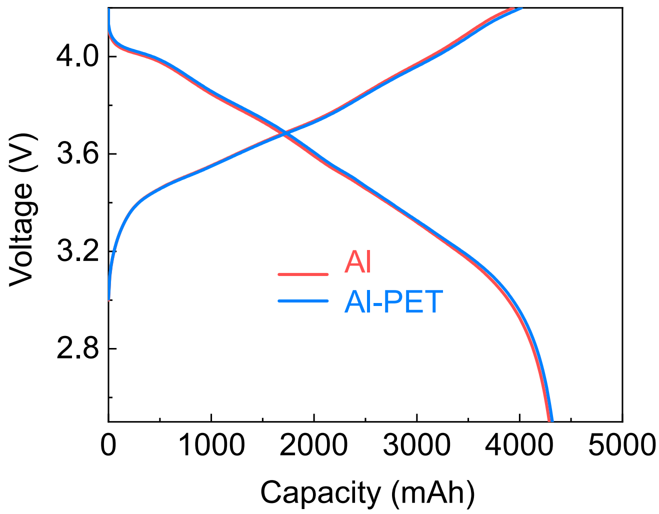

Supplementary Figure S8 Voltage-capacity curves of 4.3 Ah pouch cells using Al and Al-PET SCCs at 1/3 C for both charge and discharge.

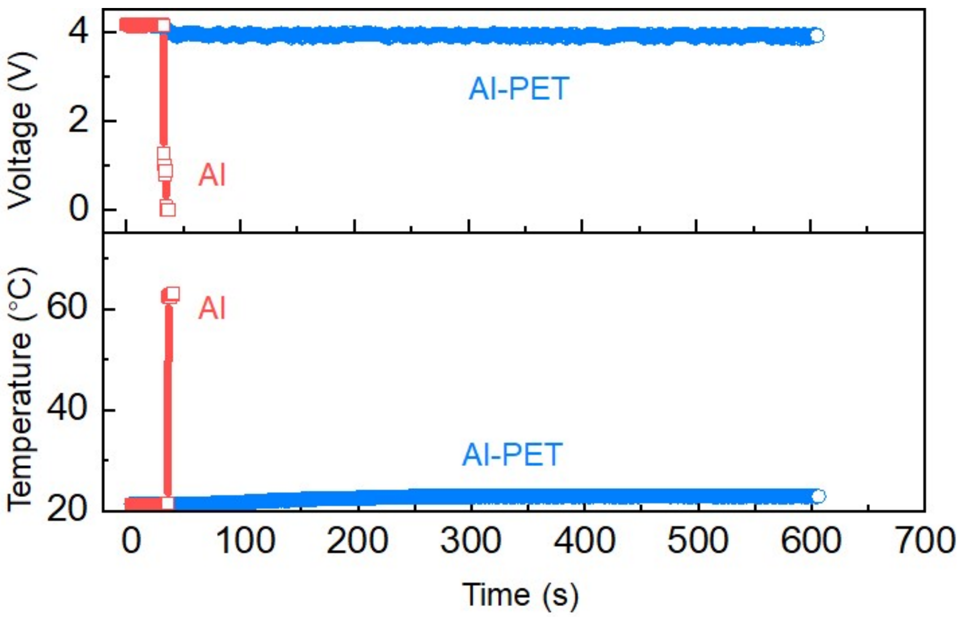

Supplementary Figure S9 Voltage and temperature (measured by a thermocouple) of 4.3 Ah pouch cells using Al-PET SCCs and Al CCs during nail penetration tests. For the cell with Al CC, only the data for the initial several seconds were recorded due to the explosion of the cell.

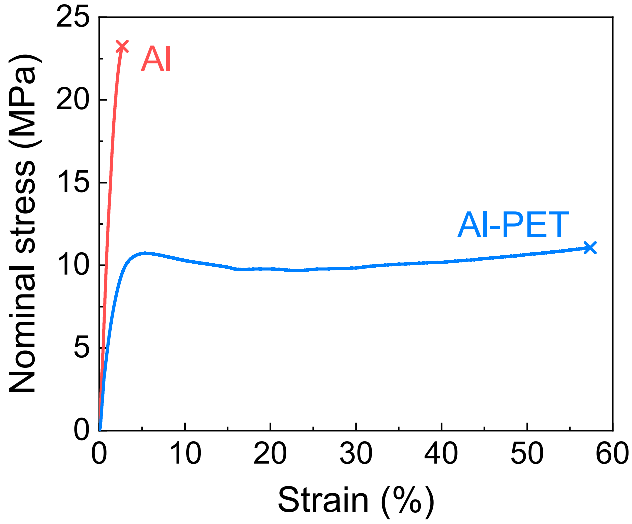

Supplementary Figure S10 Stress-strain curves of calendered cathodes (double-side coated with NCM523) using Al and Al-PET SCCs.

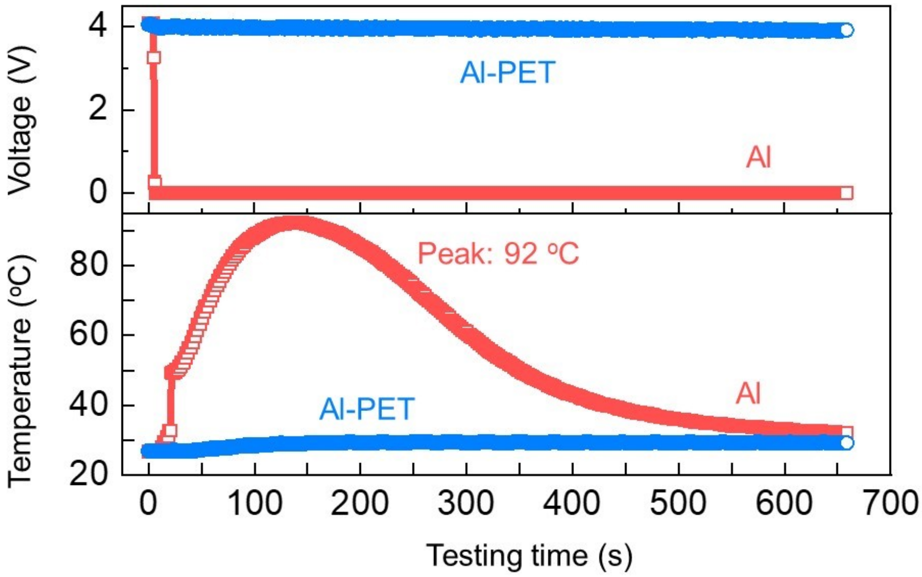

Supplementary Figure S11 Voltage and temperature (measured by a thermocouple) of 244 mAh pouch cells using Al and Al-PET SCCs during glass nail penetration test.

Supplementary Table S1 Details for 244 mAh pouch-cell specifications.

		Al CCs	Al-PET SCCs
Cell capacity (mAh)		244	
Cell weight (g)		4.684	4.556
Gravimetric energy density (Wh kg^{-1}) at 0.2C		191.3	197.0
Cathode	Active material	NCM523	
	Active material percentage (wt%)	96.2	
	Area weight excluding CC (each side, mg cm^{-2})	21.6	
	Area capacity (each side, mAh cm^{-2})	3.22	
	Length (mm)	184	
	Width (mm)	23.5	
Anode	Active materials	Graphite	
	Active material percentage (%)	96	
	Area weight excluding CC (each side, mg cm^{-2})	10.5	
	Area capacity (each side, mAh cm^{-2})	3.57	
	Length (mm)	209	
	Width (mm)	24	
Negative to positive capacity ratio		1.1	
Thickness of separator (μm)		16	
Thickness of packing foil (μm)		113	
Electrolyte to capacity ratio (g Ah^{-1})		3.3	
Weight of Al tab (g)		0.0227	
Weight of Ni Tab (g)		0.0424	

Supplementary Table S2 Details for 4.3 Ah pouch-cell specifications.

		Al CCs	Al-PET SCCs
Cell capacity (mAh)		4300	
Cell weight (g)		57.76	55.76
Gravimetric energy density (Wh kg^{-1})		263.67	270.80
Cathode	Active material	NCM811	
	Active material percentage (wt%)	97.0	
	Area weight excluding CC (each side, mg cm^{-2})	21.8	
	Area capacity (each side, mAh cm^{-2})	3.74	
	Length (mm)	80	
	Width (mm)	60	
Anode	Active materials	Graphite/SiO (15 wt%)	
	Active material percentage (%)	95.9	
	Area weight excluding CC (each side, mg cm^{-2})	8.65	
	Area capacity (each side, mAh cm^{-2})	3.5	
	Length (mm)	84	
	Width (mm)	63	
Layer of cathodes		12	
Layer of anodes		13	
Negative to positive capacity ratio		1.12	
Thickness of separator (μm)		20	
Thickness of packing foil (μm)		152	
Electrolyte to capacity ratio (g Ah^{-1})		2.3	
Weight of Al tab (g)		0.3	
Weight of Ni Tab (g)		0.9	

Supplementary Table S3 Comparison for short circuit testing between the Al//Cu and Al-PET//Cu materials. These cells were rolled by using the same cathodes and anodes as the normal pouch cells, but without electrolyte. Then the nail penetration was carried out based on the previous methods, and the resistance was recorded by using the Battery Resistance Meter (BT3562-01, HIOKI). To ensure that the shape after penetrating is not broken, the nail was pulled out along the direction of penetrating. Besides, in order to more intuitively reflect the contribution of resistance to heat, we calculated the reciprocal of the average value of resistance.

Materials		Testing conditions	Resistance (Steel nail) mΩ	$1/R_{ave}$	Resistance (Glass nail) mΩ	$1/R_{ave}$
Batteries without electrolyte	Al/Cu (NCM/Gr)	Before penetration	∞		∞	
		After penetration	57.6±25	1.74E−2	23.9±4.0	4.18E−2
		Remove the nail	297.8±81.8	3.36E−3	36.7±8.8	2.72E−2
	Al-PET/Cu (NCM/Gr)	Before penetration	∞		∞	
		After penetration	5200±1360	1.92E−4	6150±725	1.63E−4
		Remove the nail	15700±760	6.37E−5	18800±3300	5.32E−5

Supplementary Table S4 Comparison for short circuit testing between the Al//Cu and Al-PET//Cu materials. These cells were rolled by using totally different cathodes and anodes without electrolyte. To prepared the differentiated electrodes, the CCs were coated by Al_2O_3 and PVDF with a ratio of 9 : 1, and the thicknesses of electrodes were kept to consistent with normal electrodes (~130 μm for cathode, ~140 μm for anode). Then the nail penetration and the resistance record were based on the previous methods.

Materials		Testing conditions	Resistance (Steel nail) mΩ	$1/R_{ave}$	Resistance (Glass nail) mΩ	$1/R_{ave}$
Rolled CCs coated by Al_2O_3	Al/Cu (Al_2O_3/Al_2O_3)	Before penetration	∞		∞	
		After penetration	159.4±137.3	6.27E−3	74.7±70.2	1.34E−2
		Remove the nail	133±94.5	7.52E−3	57±11.3	1.75E−2
	Al-PET/Cu (Al_2O_3/Al_2O_3)	Before penetration	∞		∞	
		After penetration	∞		∞	
		Remove the nail	∞		∞	

Supplementary Table S5 Detailed information of PET (Toray Co. LTD) used in the present work. (MD denotes machine direction. TD denotes transverse direction. Ra denotes arithmetic mean roughness.)

Parameter/Properties		Unit	Measured value	Test methods
Thickness		μm	6	Micrometer
Tensile strength	MD	MPa	380	ASTM-D882-02
	TD	MPa	266	
Elongation at fracture	MD	%	87	
	TD	%	133	
Heating shrinkage	MD	%	2.9	TAK method (150 ^{o}C/30 min)
	TD	%	0.7	
Surface toughness	Ra	μm	0.072	JIS-B0601
Haze		%	6.8	ASTM-D1003
Total luminous transmission		%	88.1	

Captions for Supplementary Videos

Supplementary Video S1 Nail penetration experiment of a ~4.3 Ah pouch cells using $LiNi_{0.8}Co_{0.1}Mn_{0.1}O_2$ (NCM811) cathode and hybrid graphite@SiO anode using Al CCs under 100% state of charge. It quickly caught fire and exploded as the nail penetrated.

Supplementary Video S2 Nail penetration experiment of a ~4.3 Ah pouch cells using $LiNi_{0.8}Co_{0.1}Mn_{0.1}O_2$ (NCM811) cathode and hybrid graphite@SiO anode using Al-PET CCs under 100% state of charge. No fire or smoke were noted.

Supplementary Video S3 Roll-to-roll production of Al-PET SCCs.

Supplementary Video S4 Tensile test of cathode-coated Al CCs.

Supplementary Video S5 Tensile test of cathode-coated Al-PET SCCs. Electrical conductivity was measured at the same time.

Supplementary Video S6 Fly-by movie (around the penetration spot) of nail-penetrated cell using Al CCs by X-ray micro-computed tomography.

Supplementary Video S7 Fly-by movie (across the penetration spot) of nail-penetrated cell using Al CCs by X-ray micro-computed tomography.

Supplementary Video S8 Fly-by movie (around the penetration spot) of nail-penetrated cell using Al-PET SCCs by X-ray micro-computed tomography.

Supplementary Video S9 Fly-by movie (across the penetration spot) of nail-penetrated cell using Al-PET SCCs by X-ray micro-computed tomography.